Electronic Supplementary Material (ESI) for Nanoscale.
This journal is © The Royal Society of Chemistry 2018

SUPPLEMENTARY INFORMATION

Hierarchical nanopores by block copolymer lithography on surfaces of different materials pre-patterned by nanosphere lithography

Katharina Brassat *[a, b], Daniel Kool [a, b], Julius Bürger [a, b] and Jörg K. N. Lindner *[a, b]

---

a. *Dept. of Physics, Paderborn University, Warburgerstr. 100, 33098 Paderborn, Germany.*
b. *Center for Optoelectronics and Photonics Paderborn (CeOPP), Warburgerstr. 100, 33098 Paderborn, Germany.*
E-Mail: katharina.brassat@upb.de; lindner@physik.upb.de

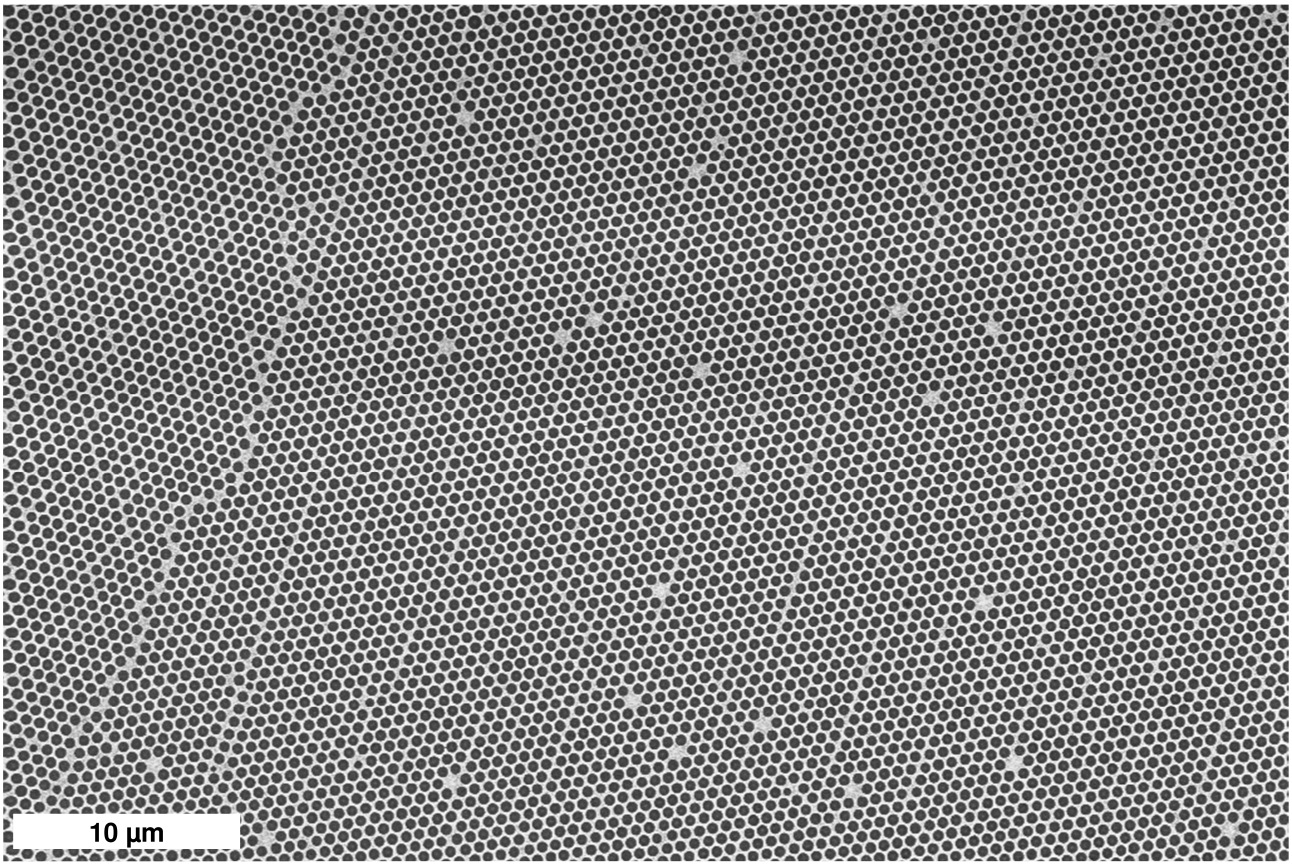

Figure S1: Low-magnification SEM image of an Au-antidot film.

Figure S1 displays a low-magnification SEM image of an antidot film formed by self-assembly of a nanosphere mask of 618 nm polystyrene spheres, followed by reactive ion etching to shrink the spheres, electron beam evaporation of 2 nm Ti and 30 nm Au, and subsequent removal of the PS mask in THF.

Figure S2 shows SEM images of sputter-deposited platinum antidots with site-selective block copolymer nanopores. The rims of the antidots are barely visible, as they have a small wall slope caused by their preparation via sputter deposition. The free SiO_2 substrate areas in the center of the antidots can be observed as dark grey dots due to material contrast (Figure S2 (a)). In order to determine the exact positions and diameters of the antidots, SEM images from the same sample position were taken with an in-lens detector, in which the nanopores are visible as in Figure S2 (a), and with an backscattered electron detector, where the Pt gives a strong material contrast (Figure S2 (b)). The overlay of both SEM images (Figure S2 (c)) then allows to determine the antidot diameter and position at which nanopores are formed inside the antidots. An exemplary antidot rim is marked in Figures S2 (a-c) (red dotted line).

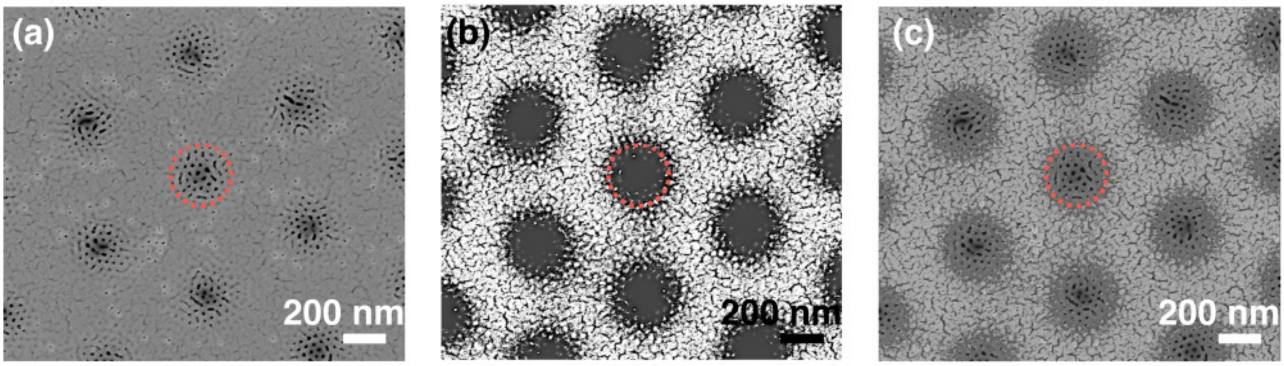

Figure S2: SEM images of site-selective BCP nanopore formation inside sputter-deposited Platinum antidots. SEM images taken with (a) an in-lens detector, (b) an backscattered electron detector and (c) an overlay of (a) and (b) allowing for the estimation of the antidot diameter.

In order to investigate if the site-selective nanopore formation inside antidots is influenced by the materials deposition technique used to create the antidot pattern we made a test sample with antidots in a 33 nm thick electron beam evaporated titanium film with the native oxide on the surface, as in Figure 7(e), and subsequently deposited 5 nm of platinum by sputtering. This means that the topography is the same as the one in Figure 7, but the surface is covered with a sputter deposited Pt film instead of an evaporated film. Performing the BCP lithography on such a surface again results in the site-selective pore formation inside the antidots, as shown in Figure S3. Similar to the evaporated Pt antidot film in Figure 7 (c) the majority of pores stands perpendicular on the sample surface and only few pores seem to be oriented in parallel, possibly due to an incomplete phase separation process. Therefore, this experiment excludes a major influence of the PVD deposition technique used and indicates that the materials chemistry and topography are the dominating factors leading to the site-selective arrangement of vertical nanopores in antidot films.

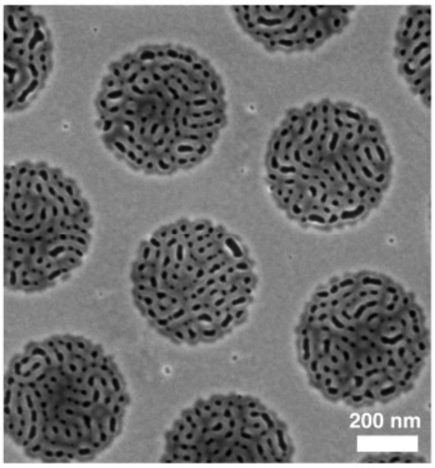

Figure S3: SEM image of site-selective BCP nanopore formation inside antidots produced by electron beam evaporation of 33 nm Ti, oxidation and subsequent sputter deposition of 5 nm Pt.

The formation of domes of nanoporous polystyrene on top of the antidot pre-patterns occurs during annealing of the BCP film. Figure S4 shows schematics of the cross-section of an Au antidot with a height of 29 nm (a) prior to BCP spin coating and (b) after BCP deposition but prior to annealing. From the reduction of antidot depth from 29 nm to 16 nm one can see that a larger amount of BCP is deposited inside the antidots than outside. Corresponding AFM measurements of evaporated Au antidots spin coated with BCP (Figure S4 (c)) do not show a dome on antidots, but a polymer film with a regular array of dimples covering the surface.

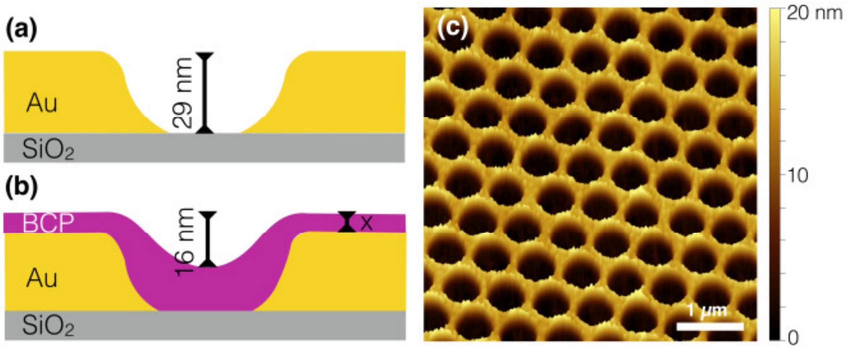

Figure S4: Wetting of antidot patterns with BCP polymer prior to annealing. Cross sectional sketch of Au antidot with height of 29 nm on a SiO_2 surface (a) without polymer film and (b) with spin casted polymer film. (c) AFM image of antidot pattern with spin coated polymer film prior to annealing. No dome is formed on top of the antidots. The height difference between antidot bottom and planar film is decreased to 16 nm as depicted in (b).

Geometrical considerations on dome formation:

The formation of a cavity underneath the domes can also be concluded from a geometrical estimation: The deposition of the polymer onto the antidot-patterned surface is performed under conditions (spin speed, polymer concentration) which result in a 30 nm thick polymer layer on a planar surface. Assuming that we spin cast a volume equivalent the total volume of polymer available for filling-up of an antidot can be estimated. If we compare this polymer volume with the volume of an antidot with cylindrical shape and geometries as in our experiment e.g. in Figure 6 (a), the polymer cylinder containing all available material would tower above the antidot film with a maximum height of 16 nm. The domes formed in our experiments however do have a height of up to 55 nm. Thus, the available amount of spin casted polymer material would not be sufficient to form such distinct domes. This fits the assumption that the antidots are most likely not completely filled with the polymer but a free standing polymer film with two air-interfaces spans over the antidot.